Adaptive Gain Changer for Precise Passivity Theory Controlled IM-DC Motor System for FEV Application

Arathy Rajeev V. K. and P. VALSALAL

***Abstract*—A passivity based control (PBC) technique is implemented for boost converter and inverter fed to induction motor coupled with DC motor. The boost converter has the advantage of giving high output voltage with less switching losses due to low operating voltage of MOSFET and low operating duty cycle. For gain optimization a feedback loop have been designed and implemented in this paper. It is found that feedback loop efficiency contributes to dynamic error detection and thereby reducing transient settling time of controller. The inverter provide reference speed to induction motor having motor torque and, load torque is applied through DC motor. The exact tracking error dynamics passive output feedback control is selected among PBC techniques as it satisfies exponential stability criteria. The system tracks the variation in speed and torque for few seconds and is verified by MATLAB/Simulink as well as field programmable gate arrays (FPGA) controller in hardware platforms.**

***Index Terms*—Boost converter, energy shaping damping injection (ESDI), exact tracking error dynamics passive output feedback (ETEDPOF), field programmable gate arrays (FPGA), full electric vehicle (FEV), induction motor (IM), passivity based control (PBC).**

Nomenclature

V_s, i_s, Ψ_s	Stator voltage, current and flux linkage vectors.
i_r, Ψ_r	Rotor current and flux linkage vectors.
R_s, R_r, L_s, L_r	Stator and rotor resistance and inductance.
M	Mutual inductance between stator and rotor.
τ, τ_m	Normalised time and overall mechanical time constant.
ω_k, ω, ω_{sR}	Angular velocity of reference frame, rotor and rated stator frequency.
Θ, N	Rotor angle and positive constant related to mass of the load and coefficient of gravity.
T_E	Generated electromagnetic torque.
J	Energy storage matrix.
R	Energy dissipation matrix.
j	Imaginary axis in s-plane.
B	Friction coefficient.
L	Inductance of converter.
C	Capacitance of converter.
u	average control input.
i	current input.
E	converter input voltage.
v	converter output voltage.
i_{am}	current input to inverter or motor current.
U	output voltage of boost converter.
D	duty cycle of boost converter.

Manuscript received June 6, 2025; revised August 22, 2025; accepted September 21, 2025. Date of publication December 30, 2025; date of current version December 2, 2025. No funding was received to assist with the preparation of this manuscript. (*Corresponding author: Arathy Rajeev V. K.*)

Both authors are with Department of EEE, CEG, Anna University, Chennai 600025, India (e-mail: arathy@student.annauniv.edu; valsalal@annauniv.edu).

Digital Object Identifier 10.24295/CPSSTPEA.2025.00035

I. Introduction

THE environmental issues caused by greenhouse gases have resulted in focusing more on energy conservation and emission reduction. Conventional fuel vehicles used for transportation is one of the major causes of emission as fuel vehicles which contribute to greenhouse gas emissions. Hence electric vehicles (EVs) are used after the development of batteries for promoting eco-friendly vehicles. The EV and hybrid electric vehicle (HEV) are more common in the market and people have started using them. The major concerns of EV are high instant power, high-power density and fast torque response [1].

The ability to operate at constant power for a wide range of speed, high efficiency and good overload performance are the major requirements of EV. These depend on battery capacity utilization, size and weight of motor as well as drive. Generally, induction motor, BLDC motor and SRM motors are widely used for EV application. Because of ruggedness, three phase induction motor is chosen for this study [2].

Generally, induction motor is less complicated, durable equipment and it runs at almost constant speed when it is controlled directly from main supply voltage. The dynamics of an induction motor is nonlinear. Even though induction motor has got many advantages, controlling of this motor, is challenging one, because rotor fluxes and currents deviate more. A passivity bend composite adaptive position control technique for induction motors is explained [3]. First, it is demonstrated that an induction motor dynamics are completely passive and a composite adaptation method is suggested to regulate position of induction motor. The passivity theory then officially establishes the global stability of induction motor position control system. Both voltage and frequency need to be changed in order to produce adjustments in speed and torque. The following insight is that voltage to frequency ratio ought to be relatively constant. Furthermore, lower efficiency and higher losses of induction motor when operating at varied speeds are main disadvantages. The demand for efficient drive systems is met by sophisticated controllers, which are not only altered losses and efficiency

but also looked for best stator current values to reduce source power consumption. The main problem is decreasing power resources which requires development of optimal controller design for electrical machines. Z. G. Wu deals with the problem of asynchronous passive control for Markov jump systems [4]. A hidden Markov model describes the asynchronization phenomena, which occurs between controller modes and system modes. The investigation demonstrates that there is a chance to reduce power consumption and increase induction motor efficiency. Drive system optimization is the term used to describe the control system, which meets all these requirements. Moreover, some optimal controllers have been developed to achieve good speed control principles while others have been created to increase accuracy and efficiency [5]. However, today's focus is on energy conservation. The energy efficiency is discussed in passivity based control (PBC), which deals with total energy of system. To offer precise monitoring of time-varying speed and flux trajectories in high magnetic saturation regions, a passivity-based controller considers saturation of magnetic material in the primary flux channel of induction motor [6]–[8].

In order to create the first wireless AC motor, a wireless shaded-pole induction motor (SPIM) skill-fully combines wireless power transmission into a single-phase SPIM [9]. The objective is to suggest a receiver self-driving circuit and drives SPIM with variable voltage and frequency. As a result, the suggested wireless SPIM gains the undeniable advantages of being completely sealable and electrocution-free. The construction of this type of induction motor is updated by Mei et al. [10]. The six-pole double-stator, double-rotor, distributed-winding axial flux induction motor with decreased back iron for electric cars is built. The design element reveals that both sets of magnetic fluxes from stator windings pass through rotor of motor without affecting them. This construction eliminates axial attractive force, and hence reducing the mechanical bearing loss. The motor is also smaller and lighter, saving more materials overall.

The total energy of the system is algebraic sum of energy stored in system and energy dissipated from the system. The desired trajectory is tracked based on Euler Lagrange equation using Hamiltonian operator [11]. The dissipation energy of the system is adjusted using a constant damping factor. A PBC method namely, exact tracking error dynamics passive output feedback (ETEDPOF) is selected to control induction motor as it tracks dynamic error which reduces the effect of transients in the system. ETEDPOF method is a simple linear time-invariant controller. The system error dynamics is plotted using Hamiltonian operator. This is stabilized by finding equilibrium points by equating the dynamics to zero. Therefore, structural dissipation matching condition is satisfied and hence asymptotically stable equilibrium points is achieved in close loop system. ETEDPOF method is preferred controller over energy shaping damping injection (ESDI) method since the controller state computation is absent. The existing control techniques are presented in Section II. The hardware controller is discussed in Section III. Problem is stated in Section IV. Proposed system is described in Section V. Proposed control method design procedure is elaborated in Section VI. Induction motor is modelled using ETEDPOF control, in Section VII. Modelling of boost converter is given in Section VIII. Software results are produced in Section IX. Comparison of proposed system with sliding mode controller (SMC) is given in Section X. Hardware results are in Section XI. Application and conclusion of research work are shown in Sections XII and XIII respectively.

II. Few Existing Control Strategies

Fault tolerant control is proposed to drive induction motor by limiting the current and voltage to a specified value [12]. A stator turn-to-turn defect detection method for induction motors operated by direct torque control for electric car powertrains is created [13]. The devised approach is based on stator currents and applying discrete wavelet transformation technique. This is a time-frequency domain-based technique which handles non-stationary signals. Zero voltage switching to turn on and zero current switching to turn off a single stage single phase isolated AC-DC converter is discussed in [14]. This converter is used for EV onboard charging with power decoupling. The design and functionality of 1-DOF (degree of freedom) and 2-DOF configurations with two controllers and associated prefilters are printed and hence the main circuit performs better than a 1-DOF structure. J. Su, R. Rao et al. [15] describe model predictive control algorithm for same EV application using induction motor. Here, the weight coefficient in cost function is adjusted for speed variations. A genetic algorithm for two stators with one rotor axial flux induction motor is discussed [16]. The machine is applied for EV and speed optimization time is better by using this genetic algorithm technique.

Due to presence of flux, current limit in an induction motor drive is not as straightforward as one in a permanent magnet motor drive. The performance of existing fault-tolerant three-phase induction motor drives has been re-examined by M. Tousizadeh [17], has taken into account, the effects of both inverter, and machine voltage limits as well as current limits. The effects of machine characteristics, operating point on voltage limit and speed limit are separated by obtaining postfault machine voltage equations. Only machine model is utilised in traditional predictive torque control (PTC) for estimating stator flux, current, and electromagnetic torque [18]. The given control technique, in contrast to conventional PTC, provides a nonlinear switching feedback element in prediction equation to deal with model errors, disturbances, and fluctuation in motor characteristics. Based on Lyapunov stability criteria, gains of feedback terms are chosen. For the purpose of estimating speed and rotor flux, an adaptive full order observer is employed. A high efficiency traction motor is designed and controlled using space vector modulation technique for achieving long driving range of EV [19]. Each open-ended phase winding in an induction motor is powered using a single H-bridge inverter. The common mode voltage and zero sequence voltage are analysed. Flux weakening is the major drawback for EV application. Recently, a study is made regarding improvement of flux, which can be extended to induction motor [20]. SMC for EV is discussed in [21]. The torque distribution coefficients are varied for dual motor EV stability. Maximum torque per ampere is

TABLE I
FEW EXISTING CONTROL STRATEGIES FOR EV USING INDUCTION MOTOR

Control methodology	Peak overshoot speed/rps	Settling time/s
Fault tolerant control	65 (Reference 50 rad/s)	0.61
Model predictive control	2500 (Reference speed 2500 rpm)	0.90
Sliding model predictive torque control	No overshoot smooth transition (Reference speed 150 rad/s)	0.45
Predictive-PI control	No overshoot smooth transition (Reference 12000 rpm)	0.61

realised in [22]. PBC is used for DC motor speed control in [23]. The motor is driven using boost converter and load torque estimation is done to eliminate speed sensors. The voltage source converter (VSC) is a linear time invariant system. PBC is used in [24] to derive control law for dual loop control method. The control algorithm is proposed for permanent magnet traction electric motor. Torque producing current and flux producing currents govern this control method. Comparison of strategies of EV are shown in Table I.

III. FIELD PROGRAMMABLE GATE ARRAYS (FPGA)

Application specific integrated circuit (ASIC) and FPGA share many of the same structural building blocks. The primary distinction between them is that FPGA has pre-set design, whereas ASIC has fixed architectures of fundamental components for different purposes [25]. Users of FPGAs can create their own digital circuits or architecture by designing and synthesising their own fields of programmable fundamental elements. In this programmable area, digital circuits are divided and operated in parallel [26]. The main advantage of FPGA is parallelism, which enables tens or even hundreds of processes to run simultaneously. The number of fundamental components is the only restriction on number of parallel circuits. The clock speed, which is ten times slower than the clock of an ASIC, is one of the numerous shortcomings. The difference is due to the fact that ASICs is tailored for speed and power consumption whereas FPGAs have general-purpose parts. The FPGA have utilised maximum clock frequency of 50 MHz and high-speed data processing, where diverse processing methods can be parallelized, and hence may be thanked for hardware description languages (HDL).

Because of their affordable volume cost and shorter time to market than other options, FPGAs are a strong solution for digital system implementation. Typically, FPGAs consist of the following features that make them more reliable and market friendly:

1) Programmable logic blocks carry out logic operations.

2) The programmable routing, that links these bit logic operations.

3) I/O blocks form off-chip connections and are coupled to logic blocks via routing interconnect.

IV. PROBLEM STATEMENT

The control of induction motor for EV application requires precise speed control for a wide range. The efficiency and performance of machine are required to be good at high speeds. The proposed controller uses less number of gain parameters, two gain values to achieve desired trajectory. Other control technique (SMC), require five gain parameter adjustment for the proposed system. Non-linear control techniques and various pulse width modulation (PWM) strategies are used to achieve speed control but control complexity is increased. Hence, nonlinearities are linearised in operating range and control law is generated using ETEDPOF method. PBC is a linear control technique which can overcome all complexities with online gain monitoring method. One of the PBC control namely ETEDPOF is proposed and voltage input is given from a boost converter to increase the efficiency. The induction motor is coupled with a DC motor as load. The controller is verified using MATLAB/Simulink model and is further implemented using FPGA hardware controller. The load torque is varied with respect to varying reference speed for thorough analysis.

V. PROPOSED SYSTEM

The block diagram of proposed system is given in Fig.1. The input is from a battery supply. If the system is connected for charging, rectifier and filter in Fig.1, will be connected to system. There is cascaded multiple supply input based on EV's mode of operation. The induction motor is triggered using an inverter. The input of inverter is controlled using boost converter which acts like a programmable DC supply. The LC filter is used to reduce the harmonics of rectified AC supply. A diode bridge rectifier is used for rectification. The gate pulses to boost converter and inverter are given from FPGA controller. The ETEDPOF control technique is used to drive induction motor, which tracks the dynamic error of state variables. For gain optimization, a feedback loop have been designed and implemented in this paper. It is found that feedback loop efficiency contributes to dynamic error detection and thereby reducing transient settling time of controller. The DC link capacitor stabilises the voltage to inverter or provides a ripple free voltage to inverter.

FPGA is selected, as one can implement parallel tasks for controlling action. In addition to control algorithm, FPGA must do other functions such as two channel high sample rate data acquisition, high-rate digital filtering on both channels, PWM modulation, command execution, and serial communication with computer to send voltage and current measurements. In Fig. 1, every activity is running in parallel with high priority. With exception of order being higher, digital filters are likewise created as transfer functions and implemented in the same manner as the controller. Digital filters' transfer functions are 4th order, regardless of order of transfer function, and the calculation speed is constant. Noises produced by high frequency switching are filtered out by filters.

Data conversion, which turns the relative value of digital data from A to D (analog to digital) converter into physical value,

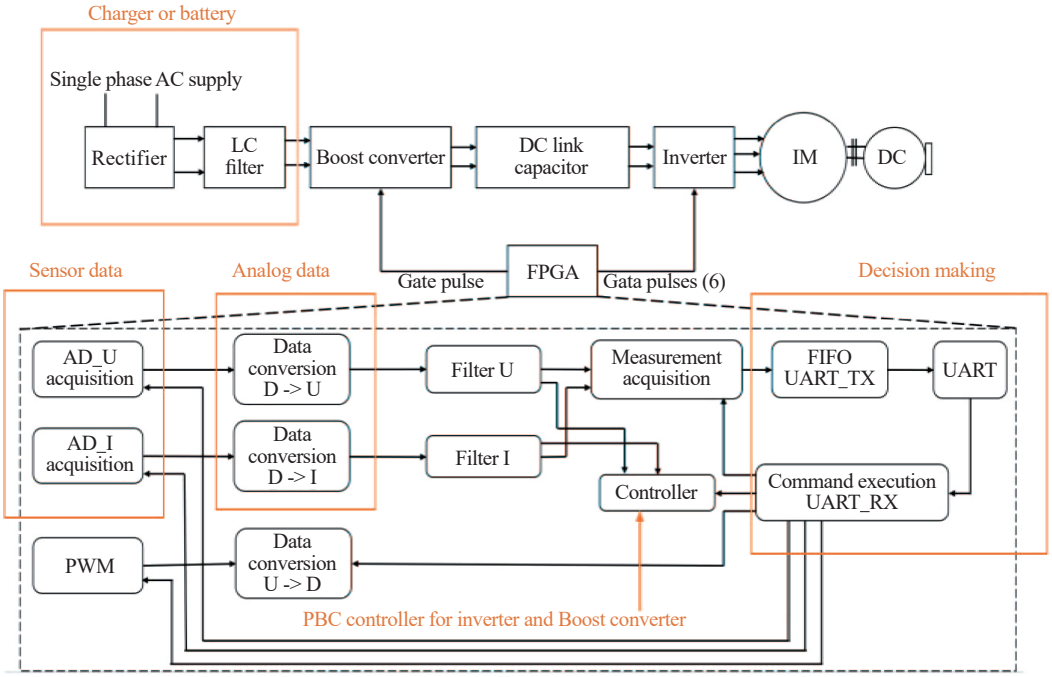

Fig. 1. Block diagram of proposed system.

is a crucial data processing step throughout the processing chain, from collection to control. Additionally, serial computer connectivity and measurement gathering are two crucial jobs. Using measurement acquisition, output voltage and inductor current of boost converter may be recorded. Samples of these measurements are then uploaded to the computer and plotted on a graph.

The proposed system is controlled using PBC based ETEDPOF controller as explained in Fig. 2. The system comprises of two power electronic converters, boost converter and inverter. The capacitor voltage and inductor current of boost converter are adjusted in such a way that whole system operates in continues conduction mode. The inverter always receives a minimum input voltage from boost converter. The induction motor is also proposed to run in a minimum of 0.5 duty cycle to reduce losses and improve steady state error. The variation in speed, start and stop of vehicle are verified using DC motor load for PBC algorithm.

The grid along with boost converter based on PBC, act as a programmable DC supply. The analysis is done using MATLAB/Simulink model and is implemented using FPGA controller in hardware. In prototype model, DC motor is connected to wheel of EV and controller gives pulse to induction motor. The power circuit and control circuit are available in controller part of the proposed system. The proposed system circuit diagram is given in Fig. 3.

Rectifier: DC supply is generated from single phase AC supply using a rectifier.

LC filter: DC harmonics present in rectified supply is eliminated with help of LC filter. The ripples in voltage are reduced below 3%.

Boost converter: The input is boosted to minimum voltage or reference voltage proportional to speed of the machine.

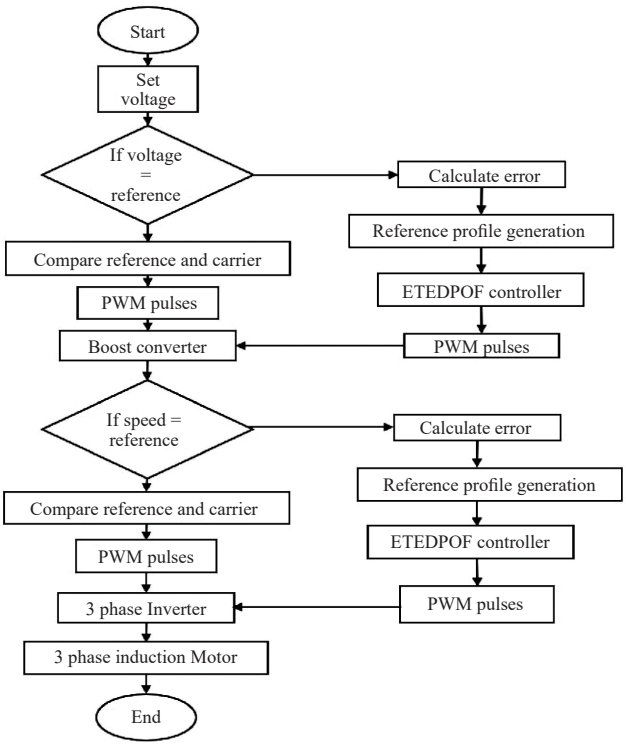

Fig. 2. Flowchart of proposed system.

Boost converter is used by considering, there is no zero-speed condition but only break condition. The system will run at minimum speed of 500 rpm always.

DC-link capacitor: The voltage is balanced and ripples are reduced using an interlink DC capacitor between two converters.

Inverter: The DC voltage is converted to AC by an inverter.

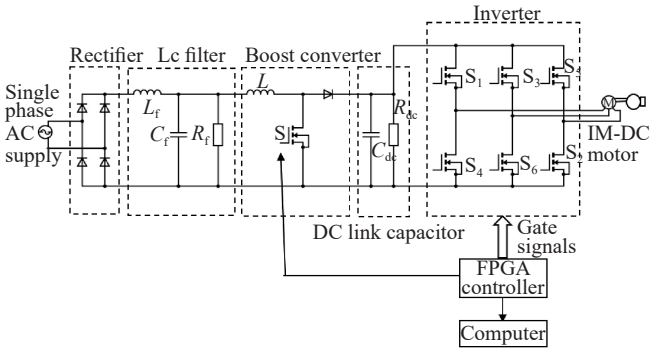

Fig. 3. Proposed system circuit diagram.

This AC supplies induction motor. The input is a varying DC according to reference speed. The gate pulses are fed from the speed observer.

IM coupled with DC motor: The wheel operation in an EV is represented by mechanical coupling of induction motor with DC motor and is used for driving a full EV (FEV).

VI. Exact Tracking Error Dynamics Passive Output Feedback Design Procedure

ETEDPOF method is used to derive control law for inverter fed induction motor. In this method, average system model characterizes exact dynamic model of stabilization error. The energy management structure of error dynamics is expressed in a generalized Hamiltonian form. So, the passive output is related to error dynamics. By identifying this error dynamics, a time invariant feedback controller is designed. According to Hebertt Sira-Ramirez et al. [2], if a dissipation matching condition is satisfied then equilibrium point will be semi-globally asymptotically stable equilibrium for a closed loop system. For control law generation, tracking of reference state trajectory with analogous reference control input trajectory is attained by

$$u - u^* = -\gamma\, \tilde{b}^{\mathrm{T}} \left[\frac{\partial H(e)}{\partial e} \right]^{\mathrm{T}} = -\gamma\, \tilde{b}^{\mathrm{T}} Me \tag{1}$$

where

$$\tilde{b} = b + \frac{\partial J(u)}{\partial u} \left[\frac{\partial H(e)}{\partial e} \right]^{\mathrm{T}} \tag{2}$$

The variations in control variable of state system are tracked by Jacobian matrix and the computed error is minimized using a Hamiltonian operator which represents energy stored in the system.

VII. Modelling of Induction Motor for EV Using ETEDPOF Method

The machine model of induction motor is given in [7].

$$V_{\mathrm{s}} = R_{\mathrm{s}} i_{\mathrm{s}} + j\omega_{\mathrm{k}} \Psi_{\mathrm{s}} + \frac{\mathrm{d}\Psi_s}{\mathrm{d}_\tau} \tag{3}$$

$$0 = R_{\mathrm{r}} i_{\mathrm{r}} + j(\omega_{\mathrm{k}} - \omega)\Psi_{\mathrm{r}} + \frac{\mathrm{d}\Psi_r}{\mathrm{d}_\tau} \tag{4}$$

where, $\Psi_{\mathrm{s}} = L_{\mathrm{s}} i_{\mathrm{s}} + M i_{\mathrm{r}}$, $\Psi_{\mathrm{r}} = L_{\mathrm{r}} i_{\mathrm{r}} + M i_{\mathrm{s}}$.

$$T_{\mathrm{e}} = |\Psi_{\mathrm{s}} \times i_{\mathrm{s}}|_{\mathrm{z}} = \tau_{\mathrm{m}} \frac{\mathrm{d}\omega}{\mathrm{d}t} + B\omega + N\sin\theta \tag{5}$$

$$\tau = \omega_{\mathrm{sR}} \times t \tag{6}$$

The above-mentioned equations are basic machine model equations of induction motor. From these equations the cartesian representation model is derived for control law generation for the proposed system.

A. Control Law Generation

The state variables are stator currents in cartesian representation i_d and i_q, which can be expressed as

$$\frac{\mathrm{d}i_d}{\mathrm{d}t} = \frac{1}{N}(V_d - e_d) \tag{7}$$

$$\frac{\mathrm{d}i_q}{\mathrm{d}t} = \frac{1}{N}(V_q - e_q) \tag{8}$$

The electromotive forces in (7) and (8) can be expressed as

$$e_d = R_{\mathrm{s}} i_d + \frac{L_{\mathrm{m}}}{T_{\mathrm{r}}}(i_d - i_{\mathrm{r}}) - (n_{\mathrm{p}}\omega + \frac{1}{T_{\mathrm{r}}}\frac{i_q}{i_{\mathrm{r}}}) Ni_q \tag{9}$$

$$e_q = R_{\mathrm{s}} i_{\mathrm{q}} + (n_{\mathrm{p}}\omega + \frac{1}{T_{\mathrm{r}}}\frac{i_q}{i_{\mathrm{r}}})(Ni_d + L_{\mathrm{m}} i_{\mathrm{r}}) \tag{10}$$

Equations have to be divided into Hamiltonian model representation to determine energy parameters, i.e., we have to separate energy dissipation and storage elements to form a state variable depending parameter which can be controlled externally. The state space model of induction motor is decomposed into J, R and M matrices as given below.

$$u = Jx + Rx + M\dot{x} \tag{11}$$

where, $\boldsymbol{J} = \begin{bmatrix} 0 & \frac{\omega_{\mathrm{e}} T_{\mathrm{r}}}{L_{\mathrm{m}}} & 0 \\ \frac{-\omega_{\mathrm{e}} T_{\mathrm{r}}}{L_{\mathrm{m}}} & 0 & 0 \\ 0 & 0 & 0 \end{bmatrix}$, $\boldsymbol{R} = \begin{bmatrix} R_\sigma & 0 & 0 \\ 0 & \frac{1}{L_{\mathrm{m}}} & 0 \\ 0 & 0 & B \end{bmatrix}$,

$\boldsymbol{M} = \begin{bmatrix} \sigma L_{\mathrm{S}} & 0 & 0 \\ 0 & \frac{T_{\mathrm{r}}}{L_{\mathrm{m}}} & 0 \\ 0 & 0 & J \end{bmatrix}$, $x = [i_{\mathrm{s}} \;\; \Psi_{\mathrm{r}} \;\; \omega_{\mathrm{m}}]$. $u = [V_{\mathrm{s}} - V_{\mathrm{b}} \;\; i_{\mathrm{s}} \; T_{\mathrm{l}}]$.

After decomposing these matrices, the stability criterion is verified. It is found that J is skew symmetric in nature and R is a symmetric matrix. Now the control law is generated from (3). The solution may be given as

$$V_{\mathrm{s}} = \gamma\,[R_\sigma i_{\mathrm{s}}^* + V_{\mathrm{b}} + R_{\mathrm{i}}(i_{\mathrm{s}}^* - i_{\mathrm{s}})] \tag{12}$$

The above control law has no integral or derivative terms. Therefore, the system control law is linear in nature. The desired trajectory of stator current converges to actual values. The damping factor is tuned nearer to system equilibrium point to

achieve desired trajectory during transient condition.

B. Reference Profile Generation

The control law in (12) is found to depend only on stator currents of induction motor. In induction motor it is represented as ratio of corresponding stator voltage and stator resistance. It can be represented as.

$$i_s^* = \frac{V_S}{R_S} \tag{13}$$

Stator current in each phase depends on torque angle based on (5). The flux in each phase is required to predict the position of rotor phase and pulses should be send to inverter switches based on rotor position.

C. Gain Optimization

The coefficients g_1 and g_2, which are obtained, may be tuned manually by trial-and-error method. Since the traditional method is time consuming, it is better to go for error profile generation of system and find system error dynamics trajectory, which is done in this paper. For any system to be stable, the dynamics is forced to nullify. This is used to find time varying gain coefficients of linear controller.

$$\dot{e} = \dot{x} - \dot{x}^* \tag{14}$$

By substituting the state space equation for actual and desired system, we obtain dynamic error trajectory of the system which is as follows:

$$\dot{e}(t) = (J - R)\left[\frac{\partial H(e)}{\partial e}\right]^{\mathrm{T}} + J\left[\frac{\partial H(x^*)}{\partial x^*}\right]^{\mathrm{T}} e_{\mathrm{u}} + \varepsilon - \varepsilon^* \tag{15}$$

where

$$e_{\mathrm{u}} = -\gamma\left[\frac{\partial H(x^*)}{\partial x^*}\right] J^{\mathrm{T}}\left[\frac{\partial H(e)}{\partial e}\right]^{\mathrm{T}} \tag{16}$$

The J matrix is independent of switching function 'u'. Therefore, e_{u} can be neglected and (15) becomes

$$\dot{e}(t) = (J - \tilde{R})\left[\frac{\partial H(e)}{\partial e}\right]^{\mathrm{T}} \tag{17}$$

where

$$\tilde{R} = \begin{bmatrix} g_1 & 0 \\ 0 & g_2 \end{bmatrix} \tag{18}$$

Substituting gain values in (18) and equating to zero, we get

$$g_1 = R_\sigma = \omega_{\mathrm{r}} L_d e_d \tag{19}$$

$$g_2 = R_{\mathrm{s}} = -\omega_{\mathrm{r}} L_q e_q \tag{20}$$

Gain parameters are found to depend on speed, self-inductance and electromotive forces generated inside an electric motor. The speed value is fed from speed sensor and will be varying instantaneously. Online adaptive gain is obtained by making current dynamics of the state equation zero. This is also similar and opposite in nature, so the supply voltage can increase or decrease with this equation. Both running and braking of EV can be controlled using this developed controller. The motor specifications are given in Table II.

TABLE II
SPECIFICATIONS OF INDUCTION MOTOR

Parameters	Values
No. of poles	4
Rated power	1000 W
Rated voltage	460 V
Rated speed	4000 rpm
Torque constant	1.2 Nm/A
Phase resistance	1.115 Ω
Phase inductance	5.974 mH
Moment of inertia	0.2×10^{-3} Nm/s^2

VIII. MODELLING OF BOOST CONVERTER SYSTEM USING ETEDPOF METHOD

The machine always runs at open loop speed and never reaches zero speed unless it is halted. Boost converter, which always has a minimum voltage, is chosen for this study based on these two criteria. Since target trajectory is a linearized model of converter system, ETEDPOF technique monitors the error more quickly. The controller now functions as a linear controller. The state space average model for boost converter is shown below.

$$L\frac{\mathrm{d}i}{\mathrm{d}t} = -(1-u)v + E \tag{21}$$

$$C\frac{\mathrm{d}v}{\mathrm{d}t} = (1-u)i - i_{\mathrm{a}} \tag{22}$$

The control law is generated for boost converter using ETEDPOF method is given as

$$U = U^* - \gamma\,(iv^* - vi^*) \tag{23}$$

The output voltage and reference values in control law are derived by equating system dynamics to zero. Therefore, reference values are derived as

$$U^* = \frac{V^*}{(1-D)} \tag{24}$$

$$v^* = k_v \omega^* \tag{25}$$

$$i^* = \frac{i_{\mathrm{a}}}{(1-D)} \tag{26}$$

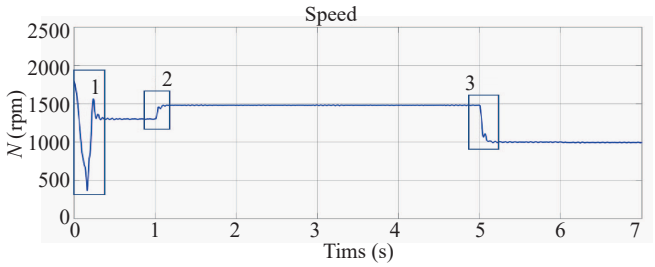

Fig. 4. Speed tracking response.

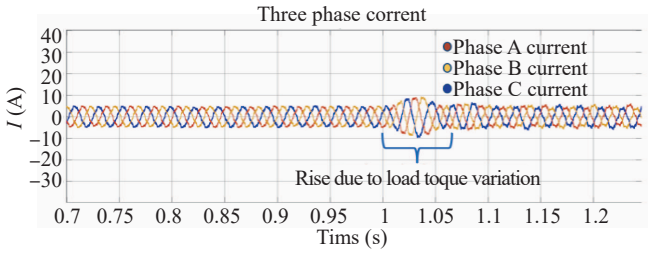

Fig. 5. Inverter input current.

The voltage reference value coming from inverter's controller output, v^* in U^*, calculates the voltage needed for anticipated speed as shown in (25). Current and voltage sensors, which are placed across passive circuit components give real values. These are two controllers used to activate converter and inverter. The simulation of system is performed based on flow chart given in Fig. 2.

IX. Results and Discussion

The grid voltage is rectified by boost converter through a LC filter to reduce harmonics injection. The converter boosts voltage to the required level according to speed trajectory of induction motor coupled with DC motor. The inverter switches as per ETEDPOF control strategy which requires state variable information from the machine. The FPGA controller updates sensor values faster compared with all other controllers so that the instantaneous error in the system is reduced.

The system is simulated in MATLAB for a step change variation of speed and load toque. The desired speed trajectory is tracked by controller in 0.2 s. Fig. 4 shows the speed trajectory in which, box 1 indicates initial inrush current suppression in 0.5 s. Box 2 represents variation in tracking desired speed given as reference in 0.2 s. Box 3 represents dip in speed, which is tracked by the controller in same time of 0.2 s. The variation in stator current of the machine due to variation in load torque is 2 A and is shown in Fig. 5. Effective electromagnetic torque generated in the machine is shown in Fig. 6, which is observed to be proportional with speed. The input voltage pulse to the inverter is given in Fig. 7 and is recorded as 600 V. The specifications of main system are given in Table III.

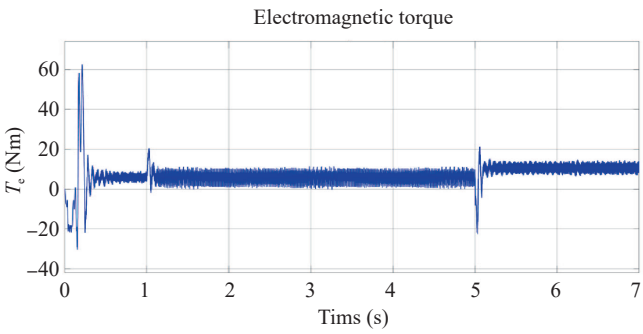

Fig. 6. Torque tracking response.

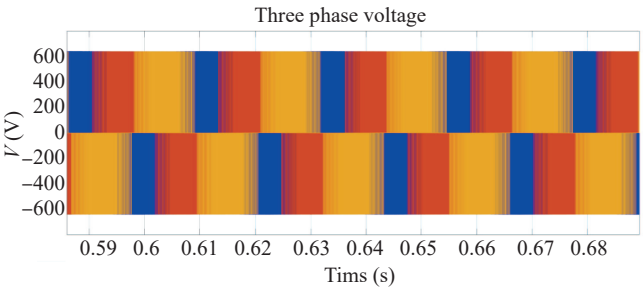

Fig. 7. Inverter input voltage.

TABLE III
Specifications of Proposed System

Circuit	Electric component	Values
LC filter	L_f	31 mH
	C_f	65 μF
	R_f	100 Ω
Boost converter	L	96 mH
DC link capacitor	C_{dc}	100 μF
	ESR	0.1 Ω
	EPR	1 Ω
	R_{dc}	100 Ω

X. Comparison of Proposed System With Sliding Mode Controller

ETEDPOF control strategy tracks a reference trajectory based on the speed change and provides proportional voltage for system to run the vehicle. The load torque variation determines change in total weight applied to motor during running of vehicle and the time it takes to track reference speed at this condition. Both systems are simultaneously run at varying speed and varying load torque condition. Speed is found to settle at 3000 rpm reference in 0.2 s without initial rise. When the gear is shifted from one to another, the speed should track a lower reference speed which is also examined. The low speed tracking of both controllers is given in Fig. 8.

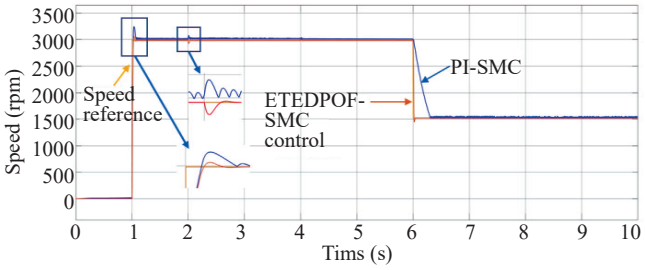

Fig. 8. Speed response for varying load torque.

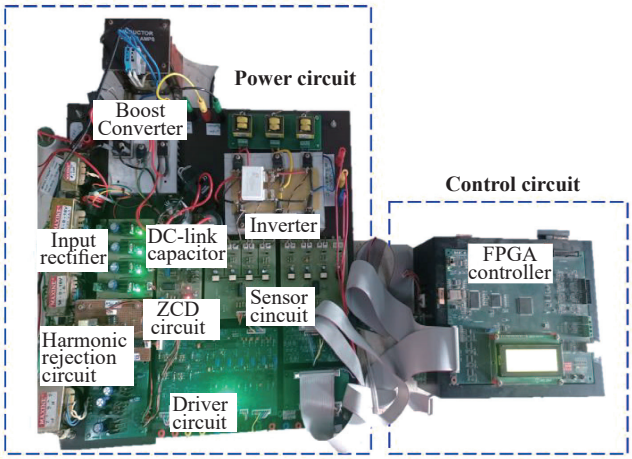

Fig. 9. Main circuit of hardware platform of the prototype for proposed system.

XI. Hardware Implementation of Proposed System

After software analysis and comparison with SMC, the system is built with FPGA controller to verify its hardware performance. The prototype hardware model is designed (Fig. 9) and simulated results are verified. The main circuit of system is understood from Fig. 9. Hardware consists of harmonic rejection circuit with inductor and capacitor circuit. Input rectifier is connected from coupling transformer to cut reverse flow of current. Main circuit consists of zero crossing detector for position estimation of rotor of induction motor.

A. FPGA Spartan 6 Driver

The controller gives signals to driver circuit of boost converter and inverter. The grid current and voltage are rectified and harmonics are reduced. The sensor voltage and current readings are recorded in DSO-X-2014A by Keysight technologies. Hardware of proposed system is built and analysed using FPGA controller using Xilinx software. The boost converter input is filtered using LC filter. The inverter input voltage is aligned by DC-link capacitor. The experimental laboratory setup is given in Fig. 10.

B. Cruise Speed Control Performance

After ripple rejection, grid current is 1.9 A as shown in Fig. 11(a). Speed reference fed to the system is shown in Fig. 11(b). It

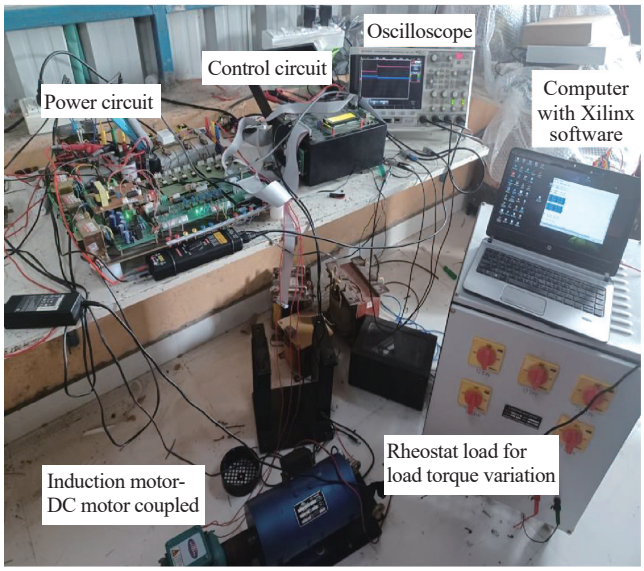

Fig. 10. Laboratory setup of proposed system.

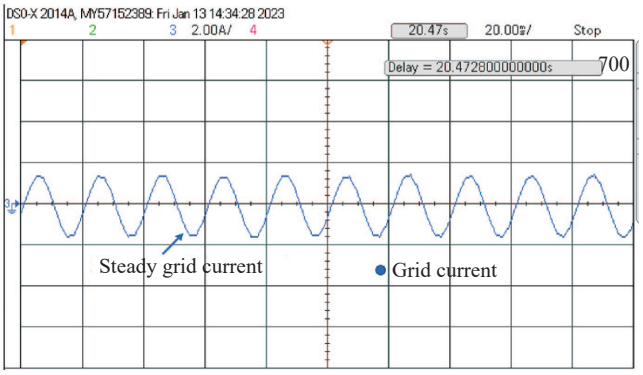

(a)

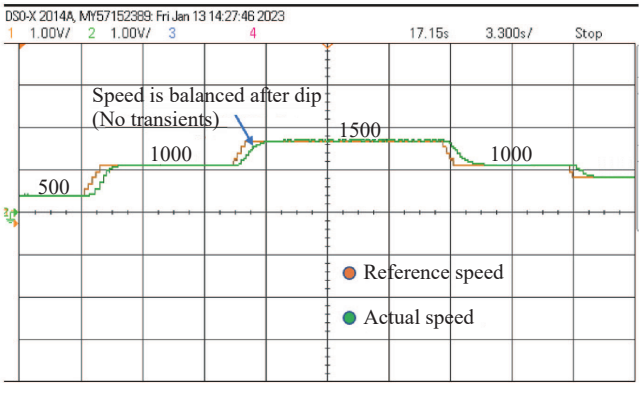

(b)

Fig. 11. (a) Grid current, (b) Reference speed tracking of ETEDPOF controller.

is variable in nature considering difficult roads other than highways for testing vehicle control efficiency. The desired speed is varied two times (2 × 500 rpm) and three times (3 × 500 rpm) as shown in Fig. 11(b) for verifying the settling time of controller which is found to be 1.2 s.

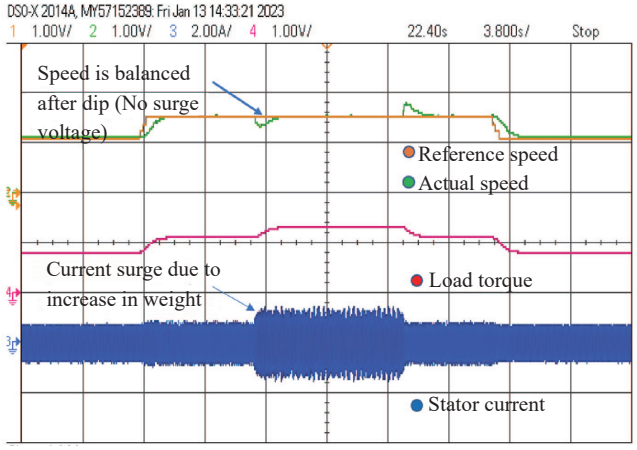

Fig. 12. Machine parameter analysis.

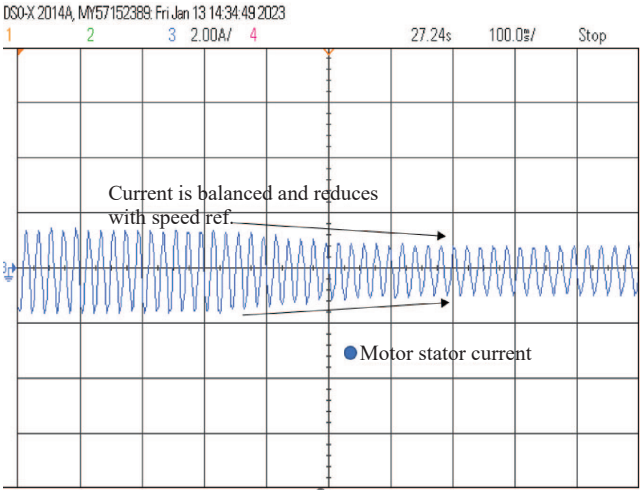

Fig. 13. Motor stator current variation with respect to load torque.

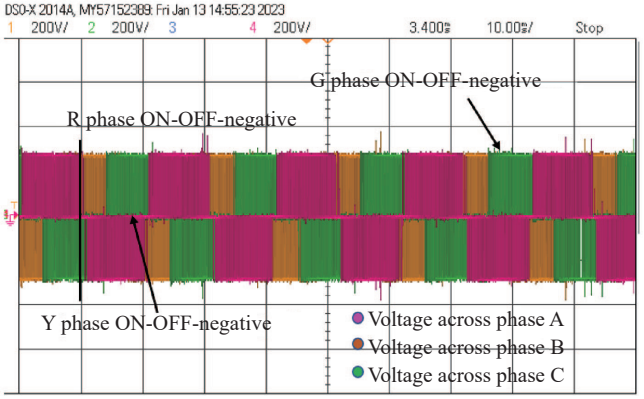

Fig. 14. Inverter output voltage.

C. Varying Load Torque Performance

In Fig. 12, speed desired value is varied from 1000 to 1500 rpm again in single step and torque is varied from 0.8,1.2 and 1.5 Nm. A ripple is found at 4.3 s where the torque is increased to 1.5 Nm and then reduced as observed in Fig. 13. The stator current of induction motor is maximum of 2.5 A and then reduced when the load torque is released. The variation of stator current when load torque is released from 1.2 Nm to 0.8 Nm is shown in Fig. 13. The respective voltage waveform is shown in Fig. 14. The three-phase current with phase shift is observed in Fig. 15. The amplitude is found to be 230 V. The line-to-line voltage of 450 V is taken across each phase and plotted using oscilloscope. This is shown separately to view the phase shift (60°) of each voltage appear across windings and is represented in Fig. 15. The voltage is a square pulse almost equal to sine wave.

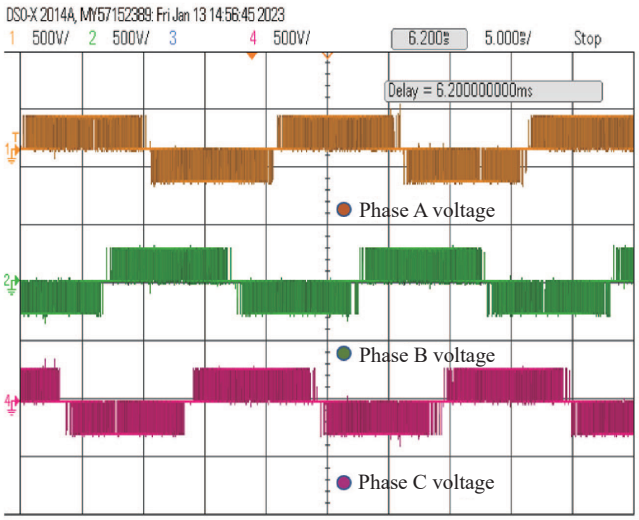

Fig. 15. Three phase induction motor input voltage.

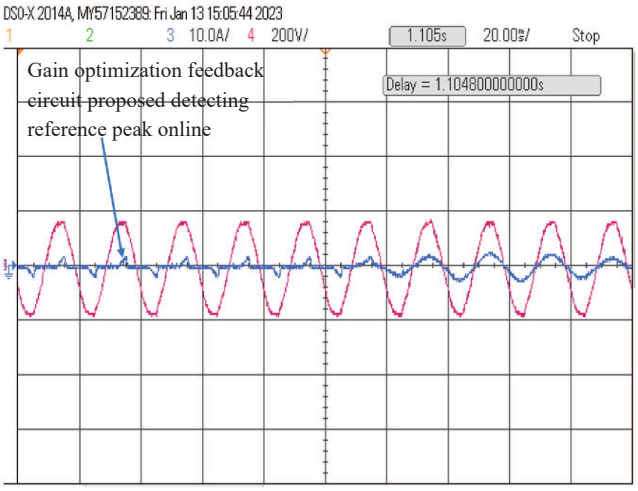

Fig. 16. Gain optimization circuit functioning waveform.

D. Proposed Online Gain Detector

The optimized gain according to (19) and (20) is implemented in hardware as feedback loops and is desired to find transient and optimum speed voltage. Fig.16 shows the controller desired peak detection according to proposed gain optimization circuit. It is also found from waveform that in online condition, the gain is optimized within 0.05 s. This will increase stability of the system.

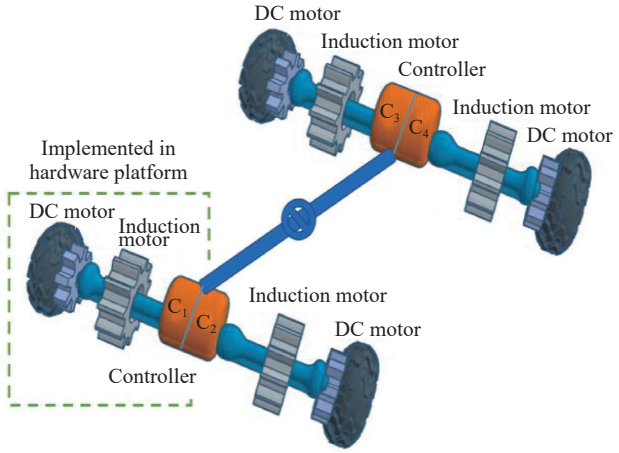

Fig. 17. Electric vehicle assembly.

XII. Application of Proposed System for EV

The settling time of speed and overshoot in voltage are less in the proposed control strategy. So, for smooth running of machine at 1500 rpm with overshoot of 1650 rpm sustained for 0.2 s and without vibration, this system is one of the best approaches for EV. The proposed controller is meant for only one wheel of EV which can be used for other three wheels for a car model as shown in Fig.17. C_1, C_2, C_3 and C_4 are controllers proposed in this work and are used for all wheels of electric car. Fig.17 represents a 3D car model, analyzed in TRICAD software to represent the proposed controller for induction motor coupled with DC motor model for electric car. ETEDPOF controller (C_1) for induction motor coupled with DC motor is connected through shaft. The same controller can be used for other three wheels for a car model.

XIII. Conclusion

Passivity based control (PBC) is an energy-based estimation technique. One of the PBC technique, ETEDPOF estimation method is used in this work. The controller tracks the speed within 0.2 s minimum and 1.2 s maximum at 1500 rpm of induction motor. A car model is presented with proposed controller for induction motor, which is coupled with DC motor. When the speed is varied from 500 rpm to 1000 rpm as well as 1500 rpm the delay in settling to reference trajectory is 0.2 s. The current transfer is smooth with very less ripple of 0.2 A and overshoot in voltage due to variation in load torque is only 10 V which is sustained for 0.2 s. In online condition, gain is optimized within 0.05 s in hardware platform. Decision making time for controller is less than 0.1 s and the initial overshoot is 0 V in hardware. This is due to soft starting strategy. The peak detection of gain circuit decides the instant of trigger. The sensor voltage and current readings are recorded in DSO-X-2014A for settling time observation. The initial reference of 500 rpm is tracked within no delay in time. The controller reduces torque ripple and therefore increases stability of the system. Using Hamiltonian operator, system state space is achieved as exponential stability. The decomposition of matrices makes system to arrive at desired trajectory settling time of 0.2 s. Hence it is desired to implement PBC for electric vehicles using induction motor. Presence of speed sensor is the limitation of this work and can be eliminated. In future, this work may be extended by using the same ETEDPOF controller technique for new converter topology. The same system can be modified to sensorless using speed observers.

Appendix I

List of Abbreviations

ASIC	Application specific integrated circuit.
BLDC	Brushless direct current motor.
DOF	Degree of freedom.
ESDI	Energy shaping damping injection.
ETEDPOF	Exact tracking error dynamics passive output feedback.
EV	Electric vehicle.
FPGA	Field programmable gate arrays.
FEV	Full electric vehicle.
HDL	Hardware description languages.
HEV	Hybrid electric vehicle.
IM	Induction motor.
PBC	Passivity based control.
PTC	Predictive torque control.
PWM	Pulse width modulation.
SMC	Sliding mode controller.
SPIM	Shaded pole induction motor.
SRM	Switched reluctance motor.
VSC	Voltage source converter.

Appendix II

Stability Analysis of PBC Method for Proposed System

A generalized Hamiltonian form is used to explain the energy management structure of error dynamics. Thus, error dynamics are connected to the passive output. The design of a time-invariant feedback controller is accomplished by recognizing these error dynamics. PBC states that the equilibrium point for a closed loop system will be a semi-globally asymptotically stable equilibrium if a dissipation matching condition is met. Equation provides the state reference trajectory of a three-phase BLDC motor supplied by an inverter:

$$\dot{x}^*(t) = (J - R)\left[\frac{\partial H(x^*)}{\partial x^*}\right]^{\mathrm{T}} + bu^* + \varepsilon \tag{27}$$

It is possible to determine the inaccuracy in system dynamics by comparing the desired and actual state spaces. For the error in system, the Hamiltonian is given as

$$H(e) = \frac{1}{2} e^{\mathrm{T}} Me \tag{28}$$

$$\frac{\partial H(e)}{\partial e} = Me = M(x - x^*) \tag{29}$$

Applying the above equation to proposed system and simplifying

$$\frac{\partial H(e)}{\partial e} = [(L_d)(i_d - i_d^*)(L_q)(i_q - i_q^*)(J)(\omega_{\mathrm{m}} - \omega_{\mathrm{m}}^*)] \tag{30}$$

For finding nature of stability of origin in error space, dynamics of the error system in (15) is given as

$$\dot{H}(e) = -\left[\frac{\partial H(e)}{\partial e}\right]\tilde{R}\left[\frac{\partial H(e)}{\partial e}\right]^{\mathrm{T}} \tag{31}$$

In the above equation, $\tilde{R}$ is dissipation matrix and is represented as

$$\tilde{R} = R + \left[b + \frac{\partial J(u)}{\partial u}\left[\frac{\partial H(e)}{\partial e}\right]^{\mathrm{T}}\right] \cdot \gamma \left[b + \frac{\partial J(u)}{\partial u}\left[\frac{\partial H(e)}{\partial e}\right]^{\mathrm{T}}\right]^{\mathrm{T}} \tag{32}$$

Since J matrix is independent on control variable 'u', the above equation reduces and value of $\tilde{R}$ is obtained as, $\tilde{R} \geqslant 0$.

Here, γ is positive damping factor and hence $\tilde{R}$ is a positive definite matrix. Now the Hamiltonian error matrix can be expressed as

$$\dot{H}(e) = -\{(R+\gamma)[(i_d - i_d^*)^2 + (i_q - i_q^*)^2] + J(\omega_{\mathrm{m}} - \omega_{\mathrm{m}}^*)\} \tag{33}$$

The equilibrium point near the origin of the error space is asymptotically stable because $\dot{H}$(e) is negative semi-definite. The outcome is not global as the control input is limited to values between 0 and 1.

References

[1] W. Wang and J.-Y. Chen, "Passivity-based sliding mode position control for induction motor drives," in *IEEE Transactions on Energy Conversion*, vol. 20, no. 2, pp. 316–321, Jun. 2005.

[2] L. U. Gokdere and M. A. Simaan, "A passivity-based method for induction motor control," in *IEEE Transactions on Industrial Electronics*, vol. 44, no. 5, pp. 688–695, Oct. 1997.

[3] W.-J. Wang and J.-Y. Chen, "Compositive adaptive position control of induction motors based on passivity theory," in *IEEE Transactions on Energy Conversion*, vol. 16, no. 2, pp. 180–185, Jun. 2001.

[4] Z. -G. Wu, P. Shi, Z. Shu, H. Su, and R. Lu, "Passivity-based asynchronous control for Markov jump systems," in *IEEE Transactions on Automatic Control*, vol. 62, no. 4, pp. 2020–2025, Apr. 2017.

[5] P. J. Nicklasson, R. Ortega, G. Espinosa-Perez, and C. G. J. Jacobi, "Passivity-based control of a class of Blondel-Park transformable electric machines," in *IEEE Transactions on Automatic Control*, vol. 42, no. 5, pp. 629-647, May 1997.

[6] F. Wang, G. Lin, and Y. He, "Passivity-based model predictive control of three-level inverter-fed induction motor," in *IEEE Transactions on Power Electronics*, vol. 36, no. 2, pp. 1984–1993, Feb. 2021.

[7] C. Cecati, "Position control of the induction motor using a passivity based controller," in *IEEE Transactions on Industry Applications*, vol. 36, no. 5, pp. 1277–1284, Sept.-Oct. 2000.

[8] C. Cecati and N. Rotondale, "Torque and speed regulation of induction motors using the passivity theory approach," in *IEEE Transactions on Industrial Electronics*, vol. 46, no. 1, pp. 119–127, Feb. 1999.

[9] H. Wang, K. T. Chau, C. H. T. Lee, L. Cao, and W. H. Lam, "Design, analysis, and implementation of wireless shaded-pole induction motors," in *IEEE Transactions on Industrial Electronics*, vol. 68, no. 8, pp. 6493–6503, Aug. 2021.

[10] J. Mei, C. H. T. Lee, and J. L. Kirtley, "Design of axial flux induction motor with reduced back iron for electric vehicles," in *IEEE Transactions on Vehicular Technology*, vol. 69, no. 1, pp. 293–301, Jan. 2020.

[11] J. Linares-Flores, J. Reger, and H. Sira-Ramírez, "Load torque estimation and passivity-based control of a boost-converter/DC motor combination," in *IEEE Transactions on Control Systems Technology*, vol. 18, no. 6, pp. 1398–1405, Nov. 2010.

[12] M. Tousizadeh, H. S. Che, J. Selvaraj, N. A. Rahim, and B. -T. Ooi, "Performance comparison of fault-tolerant three-phase induction motor drives considering current and voltage limits," in *IEEE Transactions on Industrial Electronics*, vol. 66, no. 4, pp. 2639–2648, Apr. 2019.

[13] H. H. Eldeeb, H. Zhao, and O. A. Mohammed, "Detection of TTF in induction motor vector drives for EV applications via Ostu's-based DDWE," in *IEEE Transactions on Transportation Electrification*, vol. 7, no. 1, pp. 114–132, Mar. 2021.

[14] A. Tausif, H. Jung, and S. Choi, "Single-stage isolated electrolytic capacitor-less EV onboard charger with power decoupling," in *CPSS Transactions on Power Electronics and Applications*, vol. 4, no. 1, pp. 30–39, Mar. 2019.

[15] J. Su, R. Gao, and I. Husain, "Model predictive control based field weakening strategy for traction EV used induction motor," in *IEEE Trans actions on Industry Applications*, vol. 54, no. 3, pp. 2295–2305, May-Jun. 2018.

[16] J. Mei, Y. Zuo, C. H. T. Lee, and J. L. Kirtley, "Modeling and optimizing method for axial flux induction motor of electric vehicles," in *IEEE Transactions on Vehicular Technology*, vol. 69, no. 11, pp. 12822–12831, Nov. 2020.

[17] K. V, R. Rai, and B. Singh, "Sliding model-based predictive torque control of induction motor for electric vehicle," in *IEEE Transactions on Industry Applications*, vol. 58, no. 1, pp. 742–752, Jan.-Feb. 2022.

[18] M. J. Akhtar and R. K. Behera, "Space vector modulation for distributed inverter-fed induction motor drive for electric vehicle application," in *IEEE Journal of Emerging and Selected Topics in Power Electronics*, vol. 9, no. 1, pp. 379–389, Feb. 2021.

[19] A. Credo, M. Villani, G. Fabri, and M. Popescu, "Adoption of the synchronous reluctance motor in electric vehicles: A focus on the flux weakening capability," in *IEEE Transactions on Transportation Electrification*, vol. 9, no. 1, pp. 805–818, Mar. 2023.

[20] D. Diallo, M. E. H. Benbouzid, and A. Makouf, "A fault-tolerant control architecture for induction motor drives in automotive applications," in *IEEE Transactions on Vehicular Technology*, vol. 53, no. 6, pp. 1847–1855, Nov. 2004.

[21] N. T. Dung, B. -H. Nguyen, L. H. Tran, C. D. Manh, and T. Vo-Duy, "Sliding-mode-based driving torque distribution for dynamic control of dual-motor electric vehicles," in *Proceedings of 2025 IEEE International Conference on Mechatronics (ICM)*, Wollongong, Australia, 2025, pp. 1–6.

[22] A. G. Garganeev, A. Ibrahim, and D. I. Ulyanov, "Modified algorithm for controlling the traction electric motor of a electric vehicle," in *Proceedings of 2025 IEEE 26th International Conference of Young Professionals in Electron Devices and Materials (EDM)*, Altai, Russian Federation, 2025, pp. 1260–1263.

[23] Jesús Linares-Flores, Johann Reger, and Hebertt Sira-Ramírez, "Load torque estimation and passivity-based control of a boost converter/DC-motor combination," in *IEEE Transactions on Control Systems Technology*, vol. 18, no. 6, pp. 1398–1405, Nov. 2010.

[24] Y. Liao, X. Wang, and F. Blaabjerg, "Passivity-based analysis and design of linear voltage controllers for voltage-source converters," in *IEEE Open Journal of the Industrial Electronics Society*, vol. 1, pp. 114–126, 2020.

[25] D. G. Dorrell, A. M. Knight, L. Evans, and M. Popescu, "Analysis and design techniques applied to hybrid vehicle drive machines—Assessment of alternative IPM and induction motor topologies," in *IEEE Transactions on Industrial Electronics*, vol. 59, no. 10, pp. 3690–3699, Oct. 2012.

[26] Z. Wang, T. W. Ching, S. Huang, H. Wang, and T. Xu, "Challenges faced by electric vehicle motors and their solutions," in *IEEE Access*, vol. 9, pp. 5228–5249, 2021.

Arathy Rajeev V. K. was born on July 27, 1991. She has received B.Tech. degree in Electrical and Electronics Engineering from Mahatma Gandhi University, Kerala, India in 2013, M.E degree in power electronics and drives from Anna University, Chennai, India in 2015 and currently pursuing Ph.D. at Anna University, Chennai, India. Her areas of interest include energy storage, analysis and control of electrical drives, EV.

P. Valsalal has received BE, ME and Ph.D. degrees in the year 1990,1993 and 2006 respectively. Currently she is working as Professor at College of Engineering, Guindy, Anna University. Her research area is in the field of electrical engineering. She has got around 50 research publications at her credit.